Accelerated Publications

The HPV16 E7 Viral Oncoprotein Self-Assembles into Defined Spherical Oligomers†

Leonardo G. Alonso,‡ Maria M. García-Alai,‡ Clara Smal,‡ Juan M. Centeno,‡ Rubén Iacono,§ Eduardo Castaño,§ Peter Gualfetti,|| and Gonzalo de Prat-Gay*,‡

Instituto Leloir, Facultad de Ciencias Exactas y Naturales, Universidad de Buenos Aires, Patricias Argentinas 435, (1405) Buenos Aires, Argentina, Departamento de Quimica Biologica, Facultad de Farmacia y Bioquimica, Universidad de Buenos Aires, Junin 956, C1113AAD, Buenos Aires, Argentina, and Genencor International, Inc., 925 Page Mill Road, Palo Alto, California 94304

Received November 13, 2003; Revised Manuscript Received January 15, 2004

ABSTRACT: Despite the fact that E7 is a major transforming oncoprotein in papillomavirus, its structure and precise molecular mechanism of action remain puzzling to date. E7 proteins share sequence homology and proteasome targeting properties of tumor suppressors with adenovirus E1A and SV40 T antigen, two other paradigmatic oncoproteins from DNA tumor viruses. High-risk HPV16 E7, a nonglobular dimer with some properties of intrinsically disordered proteins, is capable of undergoing pH-dependent conformational transitions that expose hydrophobic surfaces to the solvent. We found that treatment with a chelating agent produced a protein that can readily assemble into homogeneous spherical particles with an average molecular mass of 790 kDa and a diameter of 50 nm, as determined from dynamic light scattering and electron microscopy. The protein undergoes a substantial conformational transition from coil to β-sheet structure, with concomitant consolidation of tertiary structure as judged by circular dichroism and fluorescence. The assembly process is very slow, in agreement with a substantial energy barrier caused by structural rearrangements. The resulting particles are highly stable, cooperatively folded, and capable of binding both Congo Red and thioflavin T, reporters of repetitive β-sheet structures similar to those found in amyloids, although no fibrillar or insoluble material was observed under our experimental conditions.

High-risk human papillomavirus is strongly associated with cervical cancer (*1*). Papillomavirus is comprised of double-stranded DNA genomes that encode 8−10 proteins, lacking a DNA replication machinery except for DNA helicase E1 (*2*). These viruses replicate their genome by hijacking the cellular DNA replication machinery, optimaly under conditions of uncontrolled growth. Two oncoproteins, E6 and E7, cooperate for cellular immortalization (*3*, *4*), but as reported previously (*5*, *6*), the E7 open reading frame encodes the major transforming activity. In addition, HPV E7 was shown to induce DNA synthesis in quiescent cells and to cooperate with *ras* for transformation of rat kidney cells (*7*). E7 shares sequence homology with adenovirus E1A and SV40 T antigen (*8*), and this similarity extends to cell transforming activities (*5*), including interaction with key cell growth regulatory proteins such as the retinoblastoma and other pocket proteins (*9*). These proteins suppress growth through repression of transcriptional activator E2F, which is reversed by cyclin/cdk-dependent phosphorylation of Rb. E7, E1A, and SV40 T Ag can disrupt this tightly regulated network (*10*), leading to a DNA synthesis competent state, ideal for viral genome replication (*11*).

HPV16 E7 is a 98-amino acid protein with one Zn ion bound to its C-terminal domain by two highly conserved Cys-X-X-Cys motifs (*12*, *13*), coordinated in a finger-type arrangement. E7 can be phosphorylated by casein kinase II and has a short half-life in the cell cytosol (*14*). Despite its biological relevance, no structural information is available, and its function, beyond binding of a large number of reported targets, is not completely understood (*15*). The HPV16 E7 oncoprotein is a higly thermostable nonglobular dimer that undergoes a pH-dependent conformational transition that exposes hydrophobic surfaces. It shares some properties with "natively unfolded" or "intrinsically disordered" proteins (*16*, *17*), but with a stable and cooperative structure (*18*).

In the work presented here, we describe the ability of HPV16 E7 to self-assemble in the absence of zinc into defined spherical oligomers, and the characterization of these

† This work was supported by a CRP Grant (Arg 01-02) from the Institute for Genetic Engineering and Biotechnology (ICGEB, Trieste, Italy) and a PICT Grant from Agencia Nacional de promoción científica y tecnológica (PICT 01-10944). L.G.A. holds a fellowship from CONICET. G.d.P.-G. acknowledges the support from Fundacion Antorchas.

* To whom correspondence should be addressed: Instituto Leloir, Facultad de Ciencias Exactas y Naturales, Universidad de Buenos Aires, Patricias Argentinas 435, (1405) Buenos Aires, Argentina. Phone: 54-11-48658826. Fax: 54-11-48652246. E-mail: gpratgay@leloir.org.ar.

‡ Facultad de Ciencias Exactas y Naturales, Universidad de Buenos Aires.

§ Facultad de Farmacia y Bioquimica, Universidad de Buenos Aires.

|| Genencor International, Inc.

10.1021/bi036037o CCC: $27.50
Published on Web 03/02/2004

structures by electron microscopy, dynamic light scattering, and spectroscopic techniques. We discuss the likely possibility that these stable, oligomeric structures could be at least one of the forms of this protein in the cell.

MATERIALS AND METHODS

Purification of Recombinant HPV16 E7. The HPV16 E7 gene was amplified by PCR and cloned into plasmid pTZ18u under the control of the T7 promoter (*19*). The resulting plasmid was transformed into *Escherichia coli* strain BL21-(DE3) for expression. Inclusion bodies (IBs) containing HPV16 E7 were resuspended in 50 mM Tris-HCl[1] (pH 7.5), 10 mM DTT, and 8.0 M urea, then loaded onto a Q-HyperD column (BioSepra), and purified as described previously (*18*). The purified sample was dialyzed against 10 mM sodium phosphate (pH 7.0) and 1 mM DTT for storage. To obtain high-molecular mass E7 oligomers, the dimeric protein was treated with EDTA by dialyzing the protein overnight against 10 mM sodium phosphate (pH 7.0) and 1.0 mM EDTA, followed by dialysis against the same buffer without EDTA. This sample was concentrated and injected into a Superdex 200 column in 150 mM sodium phosphate (pH 7.0). The protein that eluted at the exclusion volume was collected and concentrated for storage. Inverse PCR mutagenesis was used to produce the HPV16 I93W mutant which was expressed and purified as the wild-type protein. All reagents were ACS-grade and from Sigma (St. Louis, MO) except guanidine hydrochloride (ICN).

Size Exclusion Chromatography. Gel filtration experiments were performed in a Bio-Sil SEC 250 (Bio-Rad) column in 150 mM sodium phosphate buffer (pH 7.0). E7 samples were centrifuged for 30 min at 10000*g* before injection.

Spectroscopy. Circular dichroism measurements were carried out on a Jasco J-810 spectropolarimeter. Far-UV spectra were collected using a Peltier temperature-controlled sample holder at 25 °C in a 0.1 cm path length cell, with a protein concentration of 10 μM in 10 mM sodium phosphate buffer (pH 7.0) and 1 mM DTT. Near-UV spectra of the E7 I93W mutant were collected using a 0.5 cm path length cell and a protein concentration of 54 μM in the same buffer.

Fluorescence emission spectra were recorded on an Aminco-Bowman spectrofluorimeter with an excitation wavelength of 290 nm under the conditions described in the figure legends. Thioflavin T emission spectra were recorded at excitation and emission wavelengths of 446 and 490 nm, respectively, at a protein concentration of 5 μM in 20 mM Tris-HCl (pH 8.0) and 5 μM thioflavin T. Lysozyme fibers (*20*) were used as a positive control. All reagents were filtered through a 0.2 μm filter prior to use.

For Congo Red binding experiments, a 5 μM solution of the untreated E7 protein or the E7 protein treated with EDTA was incubated for 30 min at 25 °C with 2.5 μM Congo Red in 25 mM sodium phosphate (pH 7.0). The absorbance spectrum was measured with a Jasco V-550 spectrophotometer, recording absorption from 400 to 600 nm. Lysozyme fibers were used as a positive control. All reagents were filtered through a 0.2 μm filter prior to use.

Electron Microscopy. A 40 μM aliquot of high-molecular mass soluble E7 oligomer or dimeric E7 protein was adsorbed for 1 min onto a Formvar-coated nickel grid (Electron Microscopy Science, Fort Washington, PA), then rinsed briefly with water, and negatively stained with 4% filtered aqueous sodium phosphotungstate or 2% ammonium molybdate adjusted to pH 7.0. Electron microscopy was performed with a Zeiss, EM 109 instrument.

Colorimetric Determination of the Amount of Zinc. The amount of zinc(II) was determined by spectrophotometric measurement of the level of metallochromic indicator 4-(2-pyridylazo)resorcinol (PAR) (*21*). The purified E7 dimer or oligomer without DTT was incubated with PAR (100 μM) and *p*-hydroxymercuriphenylsulfonate (PMPS) (100 μM) in 0.1 M sodium phosphate buffer (pH 7.0) for 30 min. The reaction was monitored at 500 nm, and the exact metal content was determined from a calibration curve using a Zn standard solution (Sigma). The values that were obtained are an average of two independent measurements.

Dynamic Light Scattering. Multiangle laser light scattering data were collected on a DANM DSP laser photometer emitting light at 633 nm and detecting at 18 fixed angle positions around a K5 flow cell (Wyatt Technologies, Santa Barbara, CA). Protein concentrations were determined with an OPTILAB DSP interferometric refractometer (Wyatt Technologies). Molecular mass calculations were performed on the ASTRA 4.73 software supplied with the instrument. The E7 dimer and oligomers were run in 10 mM sodium phosphate (pH 7.5) with 1 mM EDTA and 1 mM DTT, as described previously. Samples were run over a pre-equilibrated TSK-GEL G3000SWXL size exclusion chromatography column (TosoHaas) at 25 °C prior to collection of light scattering data. The protein concentration was ~60 μM in all experiments.

Phosphorylation by Casein Kinase II. Thirty microliters of 15 μM E7 and E7 oligomers were phosphorylated by incubation at 30 °C for 1 h in a buffer containing 20 mM Tris-HCl (pH 7.5), 50 mM KCl, 10 mM $MgCl_2$, and 200 μM ATP/[γ-^{32}P]ATP (200 μCi/μmol). The reaction was initiated by the addition of CKII (New England Biolabs) and stopped by heating the samples in loading buffer. Phosphorylated and control samples were subjected to SDS−PAGE (15%), and phosphate incorporation was observed by autoradiography. For gel filtration experiments, the dimeric HPV16 E7 protein was phosphorylated for 1 h at 30 °C in the described phosphorylation buffer in the presence of 200 μM ATP (same ATP/[γ-^{32}P]ATP ratio) and 250 units of CKII, with a final volume of 500 μL.

RESULTS

The HPV16 E7 Protein Self-Assembles into High-Molecular Mass Soluble Oligomers. A Zn-coordinating dimeric form of E7, obtained when refolded at high protein and DTT concentrations, is in equilibrium with the monomer at a low concentration with a K_D of 1 μM (*22*). However, high-molecular mass oligomers have been observed by slight changes in purification procedures or by expressing truncated E7 proteins (*22*, *23*). These oligomeric forms were not further

[1] Abbreviations: E7$_2$, E7 dimer; E7SOs, E7 spherical oligomers; IPTG, isopropyl 1-thio-β-D-galactopyranoside; SDS, sodium dodecyl sulfate; PAGE, polyacrylamide gel electrophoresis; DTT, dithiothreitol; PAR, 4-(2-pyridylazo)resorcinol; CKII, casein kinase II; PMPS, *p*-hydroxymercuriphenylsulfonate; GdmCl, guanidinium chloride; Tris, tris(hydroxymethyl)aminomethane; EDTA, ethylenediaminetetraacetic acid; CD, circular dichroism; Rb, tumor suppressors of retinoblastoma protein.

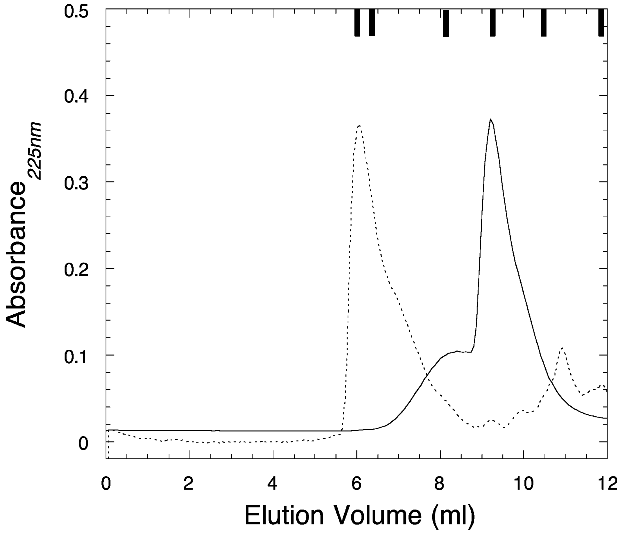

FIGURE 1: Oligomerization of HPV16 E7 by EDTA. One hundred microliters of 20 μM dimeric or EDTA-treated E7 was injected onto the gel filtration column (see Materials and Methods). The elution profiles for the EDTA-treated E7 protein (···) and dimeric E7 (—) are shown. Bars denote molecular mass standards, from left to right, with the void volume of blue dextran: 670, 158, 44, 17, and 1.35 kDa (Bio-Rad standards).

examined. In our earlier characterization, we found that EDTA could form soluble aggregates under certain conditions.

When HPV16 $E7_2$ was dialyzed against a buffer containing 1 mM EDTA subjected to gel filtration chromatography, a single peak eluting at the void volume was observed (Figure 1). These oligomers remained soluble after centrifugation for 30 min at 10000*g*. The peak corresponding to the elution volume of $E7_2$ in the absence of EDTA disappeared, indicating that the oligomerization was complete, and if the dimers were in equilibrium with E7SOs, the dissociation constant must be well below the micromolar concentration range. The oligomers remained soluble after a 30 min centrifugation at 10000*g*. Although their precise molecular mass or hydrodynamic radius cannot be inferred from this experiment, we can estimate it to be at least ~670 kDa.

Oligomers Are Defined Spherical Assemblies that Do Not Coordinate Zinc. The multiangle laser light scattering data show the major peak to have an average mass of 790 ± 7 kDa and an average radius of 26 ± 1 nm, assuming a spherical shape. A plot of radius versus elution time shows a size distribution with limited polydispersity, suggesting a fairly homogeneous size (Figure 2A). Electron microscopy shows particles with a well-defined spherical structure and a diameter of 50 ± 6 nm, in agreement with light scattering results. The apparent diameter difference in some structures within the grid could be due to differential adsorption rather than physical heterogeneity, as light scattering experiments show a nearly monodisperse sample. We named these structures E7 spherical oligomers (E7SOs). Similar results were observed when they were stained with ammonium molybdate, ruling out possible artifacts from staining conditions (not shown). When negative staining was performed with uranyl acetate (pH ~4), only amorphous aggregates were observed. No particles or aggregates were observed for $E7_2$, and no fibrous material was observed by electron microscopy under any of the conditions that were tested.

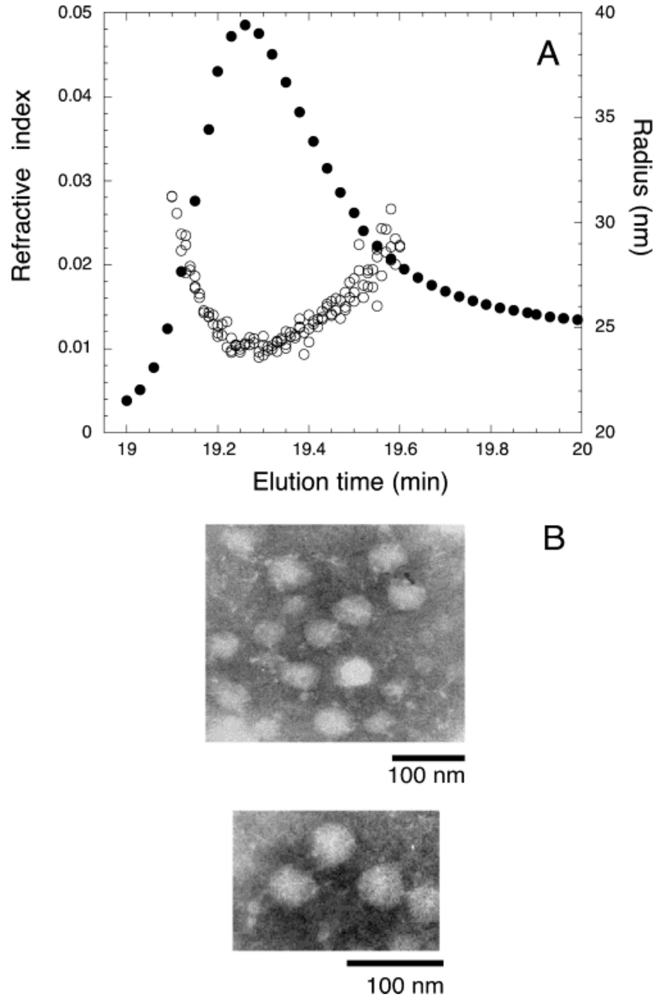

FIGURE 2: Size and shape of the oligomers. (A) Multiangle dynamic light scattering data of E7SOs. A plot of radius vs elution time shows a size distribution with limited polydispersity: refractive index (●) and radius (○) vs elution volume for E7SOs. The protein sample at 68 μM was run in 0.2 M sodium phosphate (pH 7.0) with 1 mM DTT. (B) Electron micrograph of E7SOs. The nominal magnification is 50000× for the top panel and 140000× for the bottom panel.

E7 proteins contain a zinc atom tetrahedrally coordinated to its C-terminal domain by cysteine residues 58, 61, 91, and 94 (*23*, *24*), which are essential for E7 structure and function (*13*, *25*). We quantified the metal content in the E7SOs using the PAR colorimetric assay (*21*). No zinc remained bound to the E7SO (less than 0.09 mol of zinc/mol of protein); moreover, the addition of the highly reactive thiol mercuric reagent PMPS did not increase the amount of metal detected, as in $E7_2$ (not shown). The absence of zinc and the fact that the E7SO assembly is triggered by a metal chelator strongly suggest that this process requires the release of zinc. However, we cannot exclude the possibility that other metals are involved in oligomer assembly since EDTA is a nonspecific chelator. Addition of a 20-fold excess of zinc did not dissociate the E7SOs after incubation for 24 h, even in the presence of a reductant (not shown).

The Formation of E7SOs Is Very Slow and Involves the Burial of Surface from the Solvent. The lack of tryptophan residues in HPV16 E7 prompted us to introduce such a residue so that a sensitive conformational probe would be present. An I93W mutation is fairly conserved with a tryptophan residue present in HPV18 E7, a closely related

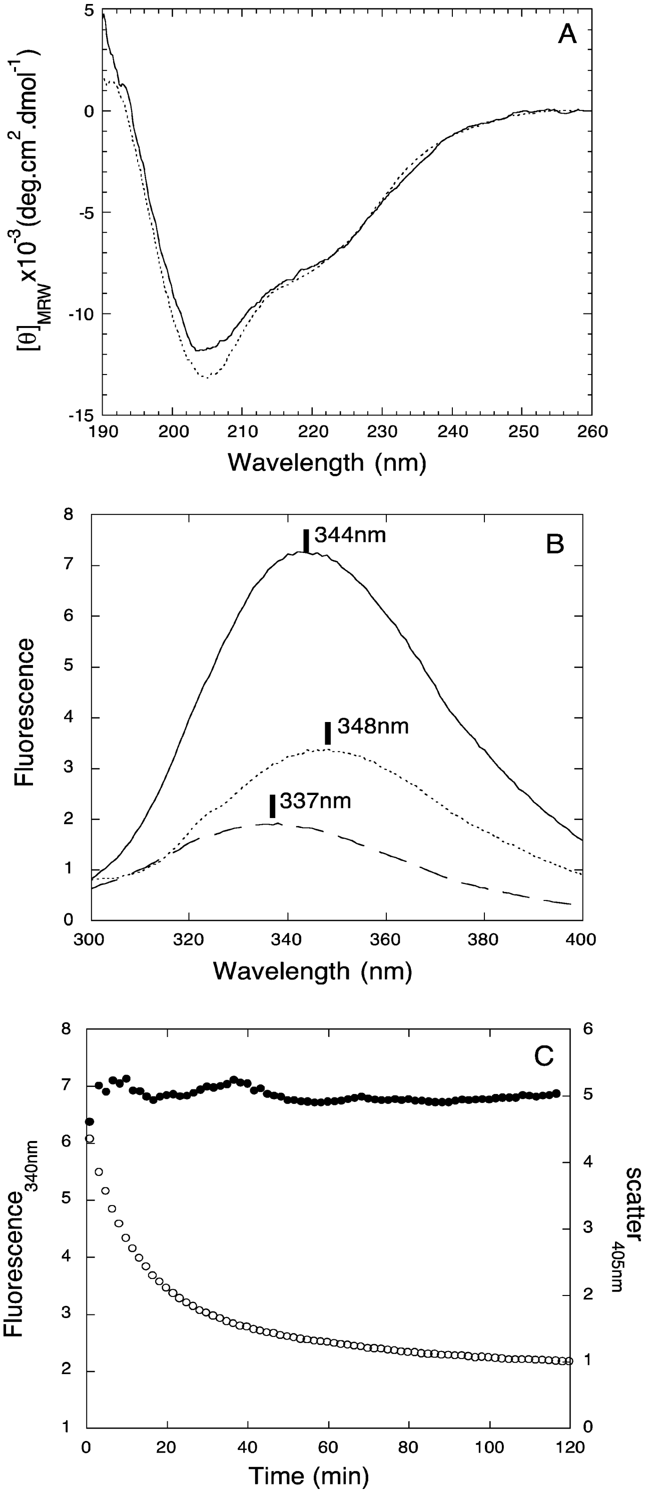

FIGURE 3: Secondary structure of E7SOs. (A) Far-UV circular dichroism spectra of the wild-type protein (—) and I93W (···). (B) Fluorescence spectra of E7SOs. Dimeric I93W (—), GdmCl-unfolded protein (···), and I93W E7SOs (− − −). (C) Kinetics of the assembly of I93W E7SOs followed by Trp fluorescence at 340 nm (excitation at 290 nmm) (○) and by light scattering at 405 nm (●). The reaction was initiated by addition of 1 mM EDTA to a protein concentration of 10 μM in 10 mM phosphate buffer (pH 7.0) at 25 °C.

high-risk strain. We confirmed that this mutation does not change either the far-UV CD spectrum (Figure 3A) or the overall stability (not shown). The blue shift in the maximum emission wavelength of the fluorescence spectrum of $E7_2$ I93W relative to that of E7SOs suggests that the trypthophan residue is partially exposed to solvent in the dimer and becomes more protected in the spherical oligomers (Figure 3B). The guanidinium chloride-unfolded E7 has a wavelength maximum of ~348 nm, which is blue shifted in the dimer to 344 nm and further shifted to 337 nm in the E7SO. I93W appears to become more buried from the solvent in the tertiary structure of the oligomers. Since I93W is placed within the zinc-coordinating motif, changes in its environment are in agreement with the metal release and a local conformational rearrangement. In addition, strong quenching of the tryptophan fluorescence is observed in the E7SOs, further supporting a change in the chromophore's environment.

Since the E7 I93W mutant displays the same behavior as the wild-type protein, judged both by CD and gel filtration experiments (data not shown), we can follow the time course of the reaction upon addition of EDTA. The kinetics of assembly were monitored by the fluorescence intensity at 340 nm and light scattering at 405 nm. The fluorescence change takes place with a half-life of 7.7 min, while light scattering remains unchanged throughout the course of the reaction (Figure 3C), suggesting that the oligomer does not aggregate.

Circular Dichroism Reveals an Increase in β-Sheet Content in the Thermostable E7SOs. The near-UV CD spectrum of HPV16 I93W, which reports on its tryptophan residue, does not show any significant band that would indicate that the chromophore is highly accessible to the solvent. A broad positive band appears in the near-UV CD spectrum of E7SOs. The changes in the environment of the aromatic residue appear to be associated with tertiary structure rearrangements, leading to at least partial burial of the side chain, coincident with the fluorescence data (Figure 4A).

The far-UV CD spectra of the dimeric wild type and I93W mutant at neutral pH exhibit a minimum at 205 nm, a band around 220 nm, and a small maximum at 190 nm (Figure 4B; *18*, *24*). In contrast, purified E7SOs show the following spectral differences. The minimum at 205 nm, which cannot be assigned unequivocally to an element of secondary structure, disappears; the maximum at 190 nm increases, and the band at ~220 nm decreases, suggesting an increase in the level of secondary structure. A differential spectrum shows a maximum centered at 195 nm and a minimum at 217 nm (Figure 4B, inset). However, the E7SO spectrum is not indicative of a pure β-sheet protein; most likely, small amounts of α-helix and other structural elements persist. The decrease in signal intensity at 205 nm simultaneously occurs with the increase in β-sheet structure content, suggesting a coil to sheet transition.

The E7 dimer is highly resistant to thermal denaturation but shows marginally cooperative changes in molar ellipticity at 220 nm upon heating (Figure 4C, inset). This behavior is compatible with the stable and extended conformation we previously described (*18*, *26*). On the other hand, E7SOs show a cooperative decrease in negative ellipticity at 220 nm, indicating a partial loss of secondary structure or that at least part of the oligomer population is being thermally unfolded. By comparing far-UV CD spectra of oligomers at 90 °C in buffer phosphate or in 6 M denaturant, we can conclude that most of the secondary structure remains unchanged at 90 °C (Figure 4C). Moreover, the shape of

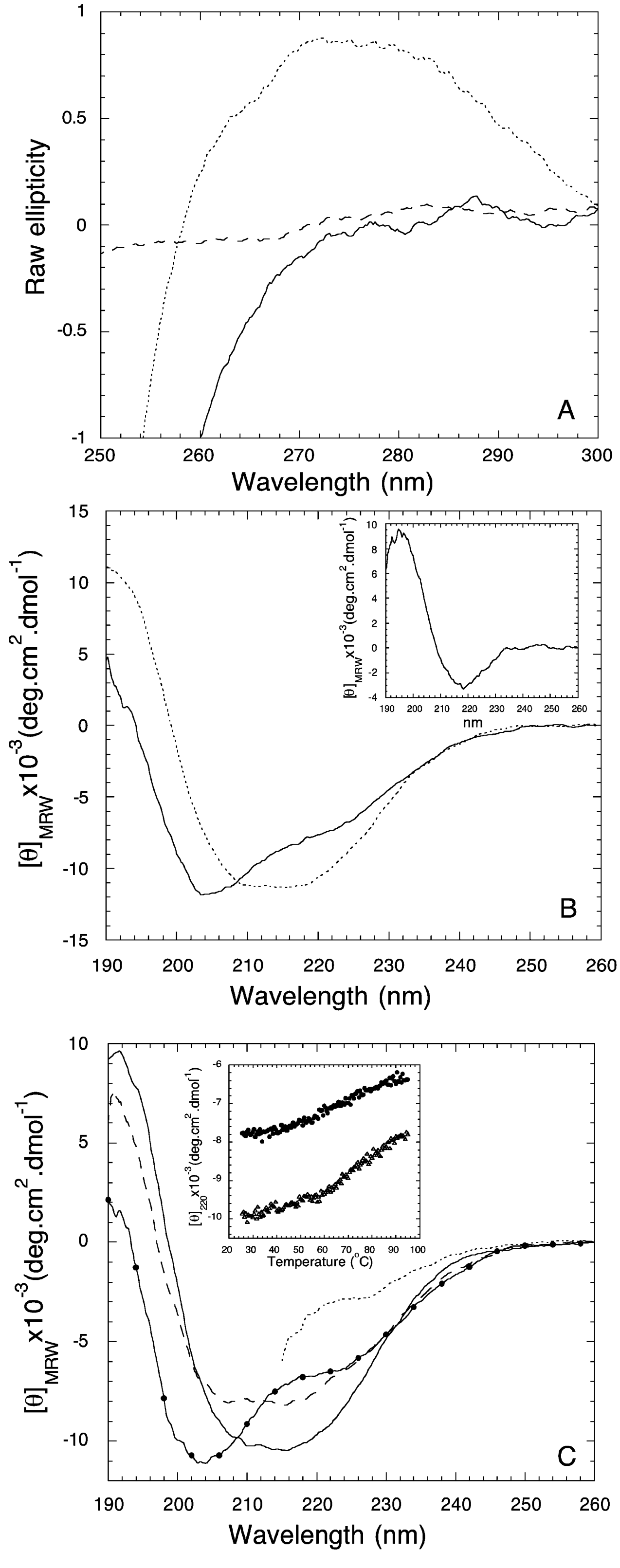

FIGURE 4: Thermostable β-sheet secondary structure induction in E7SOs. (A) Near-UV CD spectra of dimeric I93W (—), I93W E7SOs (···), and buffer (– – –). (B) Far-UV CD spectra of the dimeric wild-type E7 protein (—) and E7SOs (···). The inset shows the differential spectrum. (C) Temperature dependence of spectra. Dimeric E7 at 90 °C (—●—), E7SOs at 25 °C (—), E7SOs at 90 °C (– – –), and chemically unfolded E7SOs at 25 °C (···). No insoluble aggregates were observed after heating. The chemically unfolded protein was obtained by incubating E7SOs with 6.0 M GdmCl for 2 h. The inset shows the thermal denaturation curves of dimeric E7 (●) or E7SOs (▲).

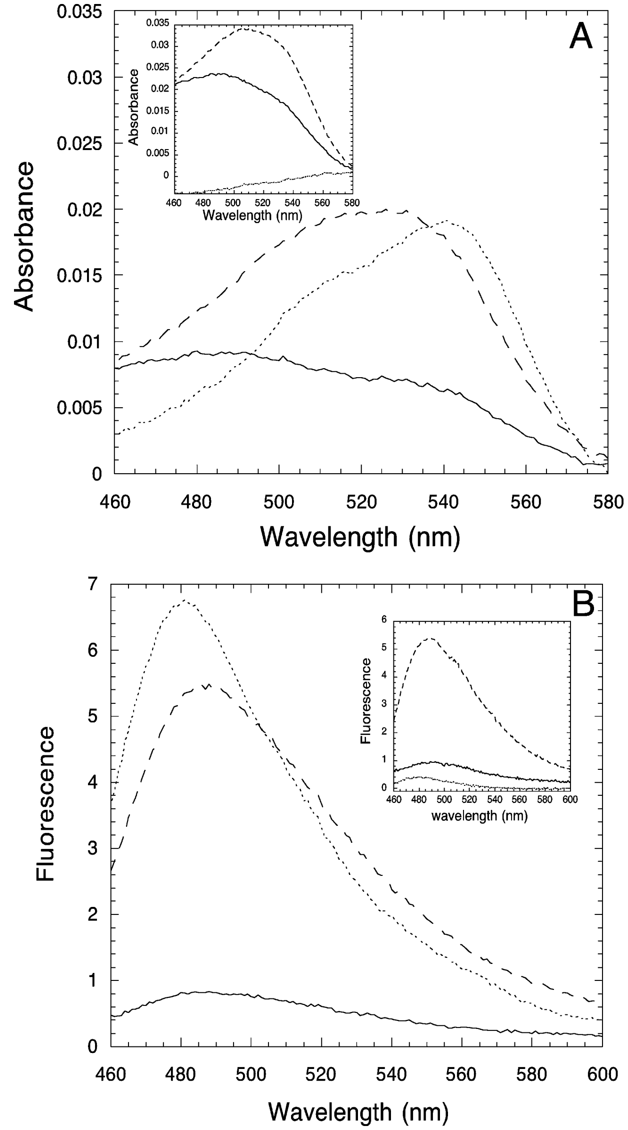

FIGURE 5: Congo Red and thioflavin binding by E7SOs. (A) Absorbance spectra of dimeric E7 (—), E7SOs (– – –), and lysozyme fibers (···) with 2.5 μM Congo Red. The inset shows the same samples, after centrifugation. (B) Thioflavin T fluorescence spectra of dimeric E7 (—), E7SOs (– – –), and lysozyme fibers (···). The inset shows the same samples, after centrifugation. Thioflavin T in buffer exhibited negligible fluorescence.

the E7SO spectrum at 90 °C is rather similar to the spectra at 25 °C and is quite different from that of the dimer at 90 °C. We can hypothesize that the secondary structures in both forms at 90 °C are qualitatively different but thermally stable.

E7SOs Bind Congo Red and Thioflavin T. The presence of a substantial increase in β-sheet content in the E7SOs prompted us to look for repetitive β-sheet structure in E7SOs, like those found in amyloid-type structures. Two of the strongest probes for these types of structures are the binding of Congo Red and the binding of thioflavin T (*27*−*29*). Absorbance spectra of E72 incubated with Congo Red show no change in either the absorbance or wavelength maximum; however, the E7SO spectrum is qualitatively and quantitatively different from that of the dimer, and resembles the positive control, lysozyme fibrils produced in vitro, with a wavelength maximum at ~530 nm (Figure 5A).

The thioflavin T fluorescence at 490 nm is largely enhanced when thioflavin T is incubated with lysozyme fibers, our positive controls, as do the E7SOs (Figure 5B). The thioflavin T fluorescence of dimeric E7 was virtually identical to that of the buffer, confirming that only the oligomers bind the dye. After centrifugation, both the Congo Red and Thioflavin T bound to E7SOs remained in the supernatant, while the lysozyme fibers precipitate as expected (insets of panels A and B of Figure 5). We can conclude that the E7SOs show amyloid-like behavior with regard to their dye binding capacity, strongly suggesting the presence of repetitive β-sheet structure, but they are clearly soluble. Nonetheless, no insoluble material was detected, in agreement with electron microscopy results.

Phosphorylation by Casein Kinase II (CKII). The E7 protein is phosphorylated by CKII at serine residues 31 and 32, which lie within the CR2 domain adjacent to the Rb binding region (*8*, *30*). The CKII recognition site is shared with CR2 of Ad E1A and SV40 T Ag. As the phosphorylation state of E7 is related to protein function, we wanted to assess if the oligomeric form could also be phosphorylated. Phosphorylation of E72 by CKII is reported by the incorporation of [^{32}P]ATP during a PAGE experiment shown in Figure 6A. Under similar conditions, the E7SOs are not phosphorylated, strongly suggesting that the phosphorylation sites are not accessible (i.e., they are buried in the oligomeric structure). E7$_2$ was phosphorylated by CKII and subsequently treated with EDTA to trigger its assembly into E7SOs, and then subjected to gel filtration chromatography. Fractions that eluted from the gel filtration column were collected, and both radioactive incorporation and the absorbance at 225 nm were found at the size of the oligomers in the exclusion volume. Therefore, the E7OSs are not phosphorylated *in vitro*, but phosphorylated E7 can assemble into oligomers. Despite the high sensitivity of the radioactive measurement, no phosphorylated dimeric E7 was detected (Figure 6B, inset), further supporting the completeness of the assembly process of the E7OSs and the high affinity of the oligomers.

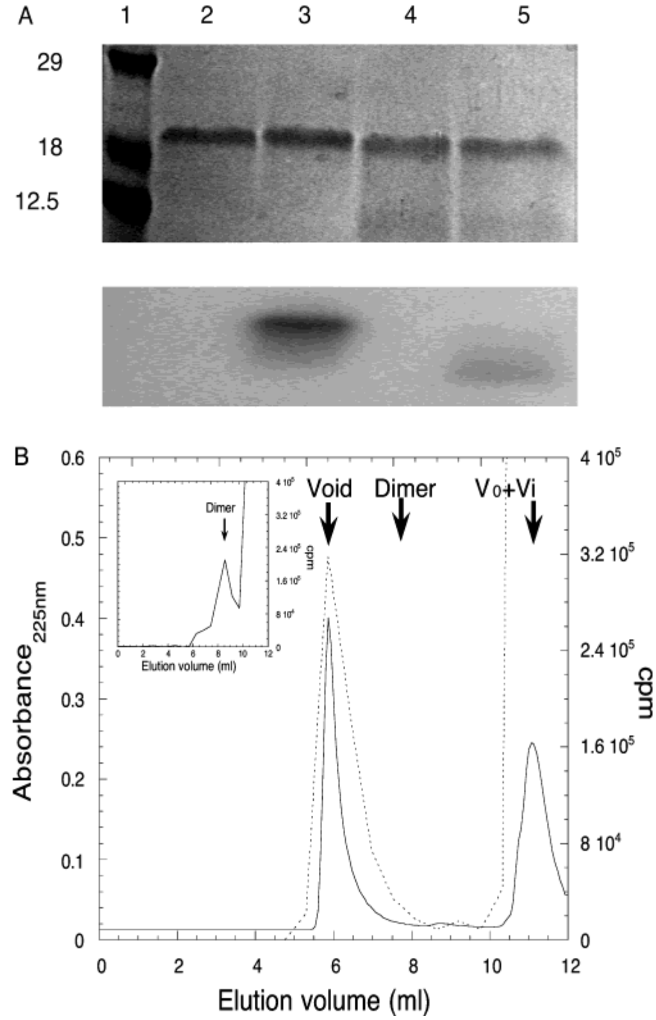

FIGURE 6: Phosphorylation of E7 and E7SOs by casein kinase II. (A) Phosphorylation of dimeric E7 and E7SOs analyzed by SDS−PAGE. The top panel shows a 15% SDS−PAGE Coomassie-stained gel (see Materials and Methods): lane 1, molecular mass markers (in kilodaltons); lane 2, dimeric E7; lane 3, dimeric E7 incubated with CKII; lane 4, E7SOs; and lane 5, E7SOs incubated with CKII. The bottom panel shows autoradiography. The amount of protein loaded onto the gel was the same for all lanes. (B) Assembly of phosphorylated dimeric E7 into E7SOs. Size exclusion chromatography of phosphorylated E7 upon EDTA treatment: absorbance at 225 nm (—) and radioactivity (···). The inset shows phosphorylated dimeric E7.

DISCUSSION

E7 is the major transforming protein of HPV16 (*5*), and it has been found to be associated with many different cellular targets (*15*, *31*). The small size of E7 may not accommodate binding sites for a large number of different tagrets. In line with this hypothesis, we have shown that its conformation is highly dependent on environmental conditions, with a particular extended conformation sharing at least some properties with intrinsically disordered or natively unfolded proteins. Alternatively, extended or apparently disordered proteins or domains may efficiently accommodate diverse target binding specificities in protein−protein interactions (*16*). In any case, no structural information leading to a defined molecular mechanism has been obtained to date for this oncoprotein, and it was always assumed that it could be only a monomer or dimer in solution. In this work, we show that dimeric HPV16 E7 can readily self-assemble "*in vitro*" into spherical oligomers (E7SOs). These are well-defined, homogeneous 50 nm particles, highly stable and cooperative, with no detectable zinc atoms present. The fact that the process can be triggered by EDTA suggests a role for the removal of zinc in the assembly.

The E7SOs cannot be phosphorylated by CKII, which shows that the phosphorylated site is not accessible or cannot be recognized by the kinase; however, the phosphorylated dimer can form E7SOs. The assembly process leaves no E7 dimer in solution, and we have not observed dissociation under any condition throughout this work, even in very dilute solutions such as those used in phosphorylation experiments. This, together with the high thermal stability, strongly suggests a very tight oligomer.

The size and morphology of E7SOs are homogeneous, and no insoluble aggregation was observed by any technique that was used. Moreover, the resulting oligomers are highly stable and cooperative, suggesting a restriction in conformational identity. When the average molecular mass of E7SOs from light scattering experiments is considered, and on the basis of the molecular mass of the E7 monomer, one E7SO molecule would contain 72 $\pm$ 1 monomers of E7.

The oligomerization involves a large increase in the level of β-sheet structure, which appears to form at the expense of the loss of disordered structure. These results further support the fact that the self-assembly of the E7 protein is an ordered, limited process, as opposed to amorphous aggregation. The observation that E7SOs can bind Congo Red and thioflavin T seems to reflect the presence of a repeated β-sheet structure, perhaps similar to that found in amyloid-like structures. However, no evidence of insoluble amyloid fibers was found in any of the electron microscopy grids that were observed, and the soluble E7SOs retain their staining properties even after centrifugation. Moreover, for a single protein molecule to assemble into a highly ordered structure, the output must necessary involve symmetry constraints (*32*, *33*). Thus, the ability to bind these probes is indicative of a repetitive β-sheet structure in the nonfibrillar self-assembly of E7SOs.

By introducing a tryptophan residue through a conservative mutation, we could observe a fluorescence quenching and a spectral shift, indicative of burial of the residue from the solvent in an asymmetric environment, confirmed by near-UV CD. This allowed us to follow the time course of assembly, which was shown to be a very slow process. This high energy barrier for assembly appears to correlate with substantial conformational changes. The availability of different probes will allow a detailed dissection of the assembly mechanism.

Other Zn binding proteins sharing RING domains, including promyelocytic leukemia protein (PML) and breast cancer susceptibility gene product 1 (BRCA 1), can self-assemble into supramolecular structures that are reminiscent of those formed in the cell, leading to bodies with polyvalent binding surfaces and scaffold partner proteins (*34*, *35*). Although E7 appears not to belong to the RING protein family because it has only one high-affinity zinc binding site, the size and shape of the E7SOs are reminiscent of several RING members. For instance, the RING domain of the promyelocytic leukemia protein (PML) can form discrete spherical multiprotein structures 0.1−1 μm in diameter (*36*). Several RING proteins can both self-assemble into spherical oligomers and promote the formation of larger multiprotein structures. Parts of the populations of HPV11 E7 and E6 were shown to colocalize with PML; however, part did not, and the apparent size of the dots appears to be heterogeneous (*37*). The sizes are not incompatible since a 50 nm sphere with a tag, two layers of antibodies used for immunohistochemistry and the intrinsic amplification of a fluorescent signal, may well yield particles with diameters of ≥ 0.1 μm.

Recently, the E6 protein from HPV16 was shown to form soluble agglomerates depending on the amount of Zn content, where the zinc was proposed to stabilize the monomeric form (*38*). Although E6 and E7 have been proposed to be evolutionarily related (*39*), it remains to be established whether they share the capacity to form soluble oligomers, and how their structures are related.

We propose that the E7 protein can change its oligomerization state and self-assemble into spherical, soluble, well-defined oligomers extending or changing its potential functions. This equilibrium is likely to be modulated by several environmental factors such as cellular differentiation, localization, pH, phosphorylation, and the levels of free zinc, which are normally very low but can otherwise influence cellular processes (*40*). This hypothesis should be confirmed *in vivo* using specific antibodies against E7SOs, which would also allow the analysis of the cellular distribution. However, there is evidence for the ability of E7 to form particles in transfected cells: low-risk HPV11 E7 was found to have a nuclear and punctuate pattern of expression in U2OS and HaCat cells (*37*). This dotlike pattern of expression was not observed for HPV16 E7, but the formation of these structures most likely will depend on the physiological state or the type of cell that is infected or transfected. In addition, the E7 proteins were tagged with a hemagglutinin epitope and developed with a-HA antibodies, and modifications in the N-terminus may also influence the formation of E7SOs.

Finally, the stability and homogeneity of the E7SOs as well as the completeness of the reaction strongly suggest that an equilibrium beyond the monomer−dimer equilibrium in HPV16 E7 must be considered. The formation of spherical oligomers containing repetitive β-sheet structure could also be considered a general architecture common to some RING or other oligomeric proteins, even if they are functionally distant.

ACKNOWLEDGMENT

We thank Andrea Gamarnik for critical reading of the manuscript.

REFERENCES

1. zur Hausen, H. (1996) Papillomavirus infections: a major cause of human cancers, *Biochim. Biophys. Acta 1288*, F55−F78.
2. Yang, L., Mohr, I., Fouts, E., Lim, D. A., Nohaile, M., and Botchan, M. (1993) The E1 protein of bovine papilloma virus 1 is an ATP-dependent DNA helicase, *Proc. Natl. Acad. Sci. U.S.A. 90*, 5086−5090.
3. Munger, K. (2002) The role of human papillomaviruses in human cancers, *Front. Biosci. 7*, d641−d649.
4. Tommasino, M., and Crawford, L. (1995) Human papillomavirus E6 and E7: proteins which deregulate the cell cycle, *BioEssays 17*, 509−518.
5. Phelps, W. C., Yee, C. L., Munger, K., and Howley, P. M. (1988) The human papillomavirus type 16 E7 gene encodes transactivation and transformation functions similar to those of adenovirus E1A, *Cell 53*, 539−547.
6. Munger, K., and Phelps, W. C. (1993) The human papillomavirus E7 protein as a transforming and transactivating factor, *Biochim. Biophys. Acta 1155*, 111−123.
7. Sato, H., Furuno, A., and Yoshiike, K. (1989) Expression of human papillomavirus type 16 E7 gene induces DNA synthesis of rat 3Y1 cells, *Virology 168*, 195−199.
8. Barbosa, M. S., Edmonds, C., Fisher, C., Schiller, J. T., Lowy, D. R., and Vousden, K. H. (1990) The region of the HPV E7 oncoprotein homologous to adenovirus E1a and Sv40 large T antigen contains separate domains for Rb binding and casein kinase II phosphorylation, *EMBO J. 9*, 153−160.
9. Dyson, N., Howley, P. M., Munger, K., and Harlow, E. (1989) The human papilloma virus-16 E7 oncoprotein is able to bind to the retinoblastoma gene product, *Science 243*, 934−937.
10. Zerfass, K., Levy, L. M., Cremonesi, C., Ciccolini, F., Jansen-Durr, P., Crawford, L., Ralston, R., and Tommasino, M. (1995) Cell cycle-dependent disruption of E2F-p107 complexes by human papillomavirus type 16 E7, *J. Gen. Virol. 76*, 1815−1820.
11. Chellappan, S., Kraus, V. B., Kroger, B., Munger, K., Howley, P. M., Phelps, W. C., and Nevins, J. R. (1992) Adenovirus E1A, simian virus 40 tumor antigen, and human papillomavirus E7 protein share the capacity to disrupt the interaction between transcription factor E2F and the retinoblastoma gene product, *Proc. Natl. Acad. Sci. U.S.A. 89*, 4549−4553.
12. Barbosa, M. S., Lowy, D. R., and Schiller, J. T. (1989) Papillomavirus polypeptides E6 and E7 are zinc-binding proteins, *J. Virol. 63*, 1404−1407.
13. McIntyre, M. C., Frattini, M. G., Grossman, S. R., and Laimins, L. A. (1993) Human papillomavirus type 18 E7 protein requires intact Cys-X-X-Cys motifs for zinc binding, dimerization, and transformation but not for Rb binding, *J. Virol. 67*, 3142−3150.

14. Smotkin, D., and Wettstein, F. O. (1987) The major human papillomavirus protein in cervical cancers is a cytoplasmic phosphoprotein, *J. Virol. 61*, 1686−1689.
15. Munger, K., Basile, J. R., Duensing, S., Eichten, A., Gonzalez, S. L., Grace, M., and Zacny, V. L. (2001) Biological activities and molecular targets of the human papillomavirus E7 oncoprotein, *Oncogene 20*, 7888−7898.
16. Dyson, H. J., and Wright, P. E. (2002) Coupling of folding and binding for unstructured proteins, *Curr. Opin. Struct. Biol. 12*, 54−60.
17. Uversky, V. N., Gillespie, J. R., and Fink, A. L. (2000) Why are "natively unfolded" proteins unstructured under physiologic conditions? *Proteins 41*, 415−427.
18. Alonso, L. G., Garcia-Alai, M. M., Nadra, A. D., Lapena, A. N., Almeida, F. L., Gualfetti, P., and Prat-Gay, G. D. (2002) High-risk (HPV16) human papillomavirus E7 oncoprotein is highly stable and extended, with conformational transitions that could explain its multiple cellular binding partners, *Biochemistry 41*, 10510−10518.
19. Mok, Y. K., de Prat Gay, G., Butler, P. J., and Bycroft, M. (1996) Equilibrium dissociation and unfolding of the dimeric human papillomavirus strain-16 E2 DNA-binding domain, *Protein Sci. 5*, 310−319.
20. Krebs, M. R., Wilkins, D. K., Chung, E. W., Pitkeathly, M. C., Chamberlain, A. K., Zurdo, J., Robinson, C. V., and Dobson, C. M. (2000) Formation and seeding of amyloid fibrils from wild-type hen lysozyme and a peptide fragment from the β-domain, *J. Mol. Biol. 300*, 541−549.
21. Hunt, J. B., Neece, S. H., and Ginsburg, A. (1985) The use of 4-(2-pyridylazo)resorcinol in studies of zinc release from *Escherichia coli* aspartate transcarbamoylase, *Anal. Biochem. 146*, 150−157.
22. Clements, A., Johnston, K., Mazzarelli, J. M., Ricciardi, R. P., and Marmorstein, R. (2000) Oligomerization properties of the viral oncoproteins adenovirus E1A and human papillomavirus E7 and their complexes with the retinoblastoma protein, *Biochemistry 39*, 16033−16045.
23. Patrick, D. R., Zhang, K., Defeo-Jones, D., Vuocolo, G. R., Maigetter, R. Z., Sardana, M. K., Oliff, A., and Heimbrook, D. C. (1992) Characterization of functional HPV-16 E7 protein produced in *Escherichia coli*, *J. Biol. Chem. 267*, 6910−6915.
24. Pahel, G., Aulabaugh, A., Short, S. A., Barnes, J. A., Painter, G. R., Ray, P., and Phelps, W. C. (1993) Structural and functional characterization of the HPV16 E7 protein expressed in bacteria, *J. Biol. Chem. 268*, 26018−26025.
25. Clemens, K. E., Brent, R., Gyuris, J., and Munger, K. (1995) Dimerization of the human papillomavirus E7 oncoprotein in vivo, *Virology 214*, 289−293.
26. Uversky, V. N. (2002) What does it mean to be natively unfolded? *Eur. J. Biochem. 269*, 2−12.
27. LeVine, H., III (1999) Quantification of β-sheet amyloid fibril structures with thioflavin T, *Methods Enzymol. 309*, 274−284.
28. Klunk, W. E., Jacob, R. F., and Mason, R. P. (1999) Quantifying amyloid by congo red spectral shift assay, *Methods Enzymol. 309*, 285−305.
29. Khurana, R., Uversky, V. N., Nielsen, L., and Fink, A. L. (2001) Is Congo red an amyloid-specific dye? *J. Biol. Chem. 276*, 22715−22721.
30. Firzlaff, J. M., Luscher, B., and Eisenman, R. N. (1991) Negative charge at the casein kinase II phosphorylation site is important for transformation but not for Rb protein binding by the E7 protein of human papillomavirus type 16, *Proc. Natl. Acad. Sci. U.S.A. 88*, 5187−5191.
31. Zwerschke, W., and Jansen-Durr, P. (2000) Cell transformation by the E7 oncoprotein of human papillomavirus type 16: interactions with nuclear and cytoplasmic target proteins, *Adv. Cancer Res. 78*, 1−29.
32. Caspar, D. L., and Klug, A. (1962) Physical principles in the construction of regular viruses, *Cold Spring Harbor Symp. Quant. Biol. 27*, 1−24.
33. Blundell, T. L., and Srinivasan, N. (1996) Symmetry, stability, and dynamics of multidomain and multicomponent protein systems, *Proc. Natl. Acad. Sci. U.S.A. 93*, 14243−14248.
34. Kentsis, A., Gordon, R. E., and Borden, K. L. (2002) Control of biochemical reactions through supramolecular RING domain self-assembly, *Proc. Natl. Acad. Sci. U.S.A. 99*, 15404−15409.
35. Kentsis, A., Gordon, R. E., and Borden, K. L. (2002) Self-assembly properties of a model RING domain, *Proc. Natl. Acad. Sci. U.S.A. 99*, 667−672.
36. Melnick, A., and Licht, J. D. (1999) Deconstructing a disease: RARalpha, its fusion partners, and their roles in the pathogenesis of acute promyelocytic leukemia, *Blood 93*, 3167−3215.
37. Guccione, E., Massimi, P., Bernat, A., and Banks, L. (2002) Comparative analysis of the intracellular location of the high- and low-risk human papillomavirus oncoproteins, *Virology 293*, 20−25.
38. Degenkolbe, R., Gilligan, P., Gupta, S., and Bernard, H. U. (2003) Chelating agents stabilize the monomeric state of the zinc binding human papillomavirus 16 E6 oncoprotein, *Biochemistry 42*, 3868−3873.
39. Cole, S. T., and Danos, O. (1987) Nucleotide sequence and comparative analysis of the human papillomavirus type 18 genome, *J. Mol. Biol. 193*, 599−608.
40. Outten, C. E., and O'Halloran, T. V. (2001) Femtomolar sensitivity of metalloregulatory proteins controlling zinc homeostasis, *Science 292*, 2488−2492.

BI036037O